HHS Public Access

Author manuscript

Immunity. Author manuscript; available in PMC 2019 June 19.

Published in final edited form as:

Immunity. 2018 June 19; 48(6): 1172–1182.e6. doi:10.1016/j.immuni.2018.04.018.

Transcription factor IRF8 orchestrates the adaptive natural killer cell response

Nicholas M. Adams[1], **Colleen M. Lau**[1], **Xiying Fan**[1], **Moritz Rapp**[1], **Clair D. Geary**[1], **Orr-El Weizman**[1], **Carlos Diaz-Salazar**[1], and **Joseph C. Sun**[1,2,3,*]

[1]Immunology Program, Memorial Sloan Kettering Cancer Center, New York, NY 10065, USA

[2]Department of Immunology and Microbial Pathogenesis, Weill Cornell Medical College, New York, NY 10065, USA

[3]Lead Contact

Summary

Natural killer (NK) cells are innate lymphocytes that display features of adaptive immunity during viral infection. Biallelic mutations in *IRF8* have been reported to cause familial NK cell deficiency and susceptibility to severe viral infection in humans; however, the precise role of this transcription factor in regulating NK cell function remains unknown. Here, we show that cell-intrinsic IRF8 was required for NK cell-mediated protection against mouse cytomegalovirus infection. During virus exposure, NK cells upregulated IRF8 through interleukin-12 (IL-12) signaling and the transcription factor STAT4, which promoted epigenetic remodeling of the *Irf8* locus. Moreover, IRF8 facilitated the proliferative burst of virus-specific NK cells by promoting expression of cell cycle genes, and directly controlling Zbtb32, a master regulator of virus-driven NK cell proliferation. These findings identify the function and cell type-specific regulation of IRF8 in NK cell-mediated antiviral immunity, and provide a mechanistic understanding of virus susceptibility in patients with *IRF8* mutations.

eTOC Blurb

The link between human *IRF8* mutations and immunodeficiency is poorly understood. Adams et al. demonstrate that IRF8 is required for NK cell-mediated antiviral immunity by promoting proliferation of virus-specific NK cells.

Graphical Abstract

*Correspondence: Joseph C. Sun, PhD, Memorial Sloan Kettering Cancer Center, 408 East 69th Street, ZRC-1462, New York, NY 10065, Phone: 646-888-3228, Fax: 646-422-0452, sunj@mskcc.org.

Author Contributions

Conceptualization, N.M.A. and J.C.S.; Data Analysis, N.M.A., C.M.L., and X.F.; Investigation, N.M.A., M.R., C.D.G., O.-E.W., and C.D.-S.; Writing – Original Draft, N.M.A. and J.C.S.; Writing – Review & Editing, N.M.A and J.C.S.; Data Visualization, N.M.A., C.M.L., and X.F.; Supervision, J.C.S.; Funding Acquisition, J.C.S.

Declaration of Interests

The authors declare no competing interests.

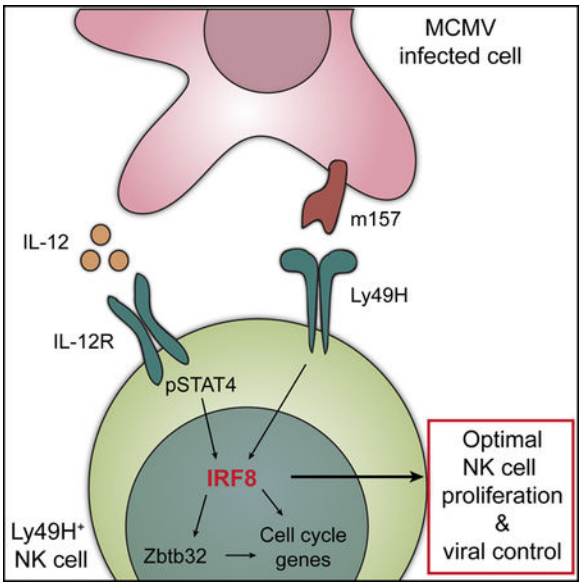

Keywords

NK cells; IRF8; viral infection; transcriptional regulation

Introduction

Natural killer (NK) cells are innate lymphocytes capable of killing stressed, transformed, or infected cells without prior sensitization (Lanier, 2005). Their germline-encoded receptor repertoire and status as poised effectors classically position NK cells as cells of the innate immune system. However, more recent evidence suggests that NK cells possess features of adaptive immunity, including their derivation, requirements for homeostatic maintenance, and acquisition of functional competence (Sun and Lanier, 2011). Recent studies demonstrate that NK cells undergo a robust burst of clonal proliferation during mouse cytomegalovirus (MCMV) infection to promote viral clearance (Daniels et al., 2001; Dokun et al., 2001; Sun et al., 2009), and establish a long-lived memory population with enhanced protective function against MCMV reinfection (Sun et al., 2009), functions thought to be limited solely to T and B cells of the adaptive immune system.

During MCMV infection, NK cells mediate this “adaptive” antiviral response by binding the viral glycoprotein m157 on infected cells with the DAP12-dependent activating receptor Ly49H (Arase et al., 2002; Daniels et al., 2001; Dokun et al., 2001; Sun et al., 2009). In addition to detection of viral ligands, these adaptive NK cell responses critically require proinflammatory cytokines, particularly interleukin-12 (IL-12), IL-18, and type I interferons, which play differential roles in supporting NK cell proliferation and survival during expansion, and imprinting the effector to memory NK cell transition (Madera et al., 2016; Madera and Sun, 2015; Sun et al., 2012). Nevertheless, the transcriptional regulators NK cells employ to integrate these signals, and the transcriptional programs they drive to generate antiviral responses, are only beginning to be elucidated.

The interferon regulatory factor (IRF) family of transcription factors consists of nine members in mammals with differential dependencies on type I and type II interferon signaling and pleiotropic functions both within and outside of the immune system (Tamura et al., 2008). Our current understanding of the requirement for IRF family members in mouse NK cell development and function is limited to IRF1 and IRF2. NK cell development is impaired in germline *Irf1*$^{-/-}$ mice (Duncan et al., 1996; Ogasawara et al., 1998; Taki et al., 1997); however, this was demonstrated to be secondary to IRF1-dependent IL-15 production by radiation-resistant bone marrow stromal cells that support NK cell development (Ogasawara et al., 1998). In contrast, IRF2 is thought to be required in a cell-intrinsic manner to support the survival of mature peripheral NK cells (Lohoff et al., 2000; Taki et al., 2005). More recently, a clinical study identified compound heterozygous or homozygous *IRF8* mutations that segregated with severe, and in some cases fatal, viral susceptibility in 3 unrelated families (Mace et al., 2017). These patients possessed a greatly diminished number of mature NK cells and reduced NK cell cytolytic function, suggesting a role for IRF8 in NK cell development and function. However, the direct *in vivo* function of IRF8 in NK cells has not been established.

Expression of IRF8 (also known as ICSBP) is restricted to the immune system, and a growing number of studies has revealed the critical and divergent roles that IRF8 plays in the transcriptional regulation of hematopoiesis and peripheral immune responses, including monocyte and dendritic cell (DC) lineage commitment (Holtschke et al., 1996; Schiavoni et al., 2002; Tamura et al., 2000), B cell development (Lu et al., 2003) and germinal center reactions (Lee et al., 2006; Xu et al., 2015), T helper-1 (Th1) cell differentiation (Giese et al., 1997; Scharton-Kersten et al., 1997), and thymic selection (Herzig et al., 2017). Given its prominent role in lymphocyte biology, and its frequent mutation in familial cases of NK cell deficiency and viral susceptibility, we hypothesized that IRF8 may act as an essential regulator of NK cell antiviral responses.

In this study, we show that the transcription factor IRF8 played a critical and non-redundant role in facilitating the proliferative burst of virus-specific NK cells during acute viral infection, but was dispensable for their development. We used conditional *Irf8* ablation to demonstrate that IRF8 was required in a cell-intrinsic manner for host protection against lethal viral challenge, consistent with the induction of IRF8 during early NK cell activation. We found that the IL-12 and STAT4 signaling axis promoted IRF8 upregulation, which drove the proliferation of antigen-specific NK cells by activating a transcriptional program that promoted cell cycle progression and expression of the pro-proliferative transcription factor Zbtb32. These findings attribute a function and regulation for IRF8 in NK cell-mediated host immunity.

Results

NK cells require IRF8 for antiviral immunity

NK cells play an essential, dominant role in control of MCMV and human cytomegalovirus (HCMV) infection in mice and humans, respectively (Biron et al., 1989; Bukowski et al., 1985; Etzioni et al., 2005). To determine whether IRF8 was required for host antiviral immunity, we first challenged wild-type (WT) and *Irf8*$^{-/-}$ mice with a lethal dose of MCMV.

Compared to WT mice, *Irf8*$^{-/-}$ mice rapidly succumbed to MCMV infection due to elevated viral burden (Figures 1A and 1B). Loss of IRF8-dependent CD8α^{+} DCs in *Irf8*$^{-/-}$ mice impairs IL-12 production (Giese et al., 1997; Scharton-Kersten et al., 1997), which is required to prime NK cells (Sun et al., 2012). Therefore, to investigate whether NK cells require IRF8 in a cell-intrinsic fashion for MCMV control, we began by generating a genetic mouse model with conditional deletion of *Irf8* exon 2 specifically in NK cells (*Nkp46*$^{iCre/+}$ *Irf8*$^{fl/fl}$, herein designated NK-*Irf8*$^{-/-}$) (Figure S1A). NK cell numbers, frequency, maturation, and receptor repertoire were unaffected by loss of IRF8 (Figures S1B–S1E), suggesting this transcription factor was dispensable during NK cell development and homeostasis. To test the protective capacity of IRF8-deficient NK cells, we challenged NK-*Irf8*$^{-/-}$ and Cre-negative littermate control mice (*Irf8*$^{fl/fl}$) with a lethal dose of MCMV. NK-*Irf8*$^{-/-}$ mice exhibited poorly controlled viral replication, and many failed to survive beyond 4 days post infection (p.i.) (Figures 1C and 1D). Thus, IRF8 is required in a cell-intrinsic manner for protective antiviral responses by NK cells.

NK cells rapidly upregulate IRF8 during MCMV infection in response to IL-12 and STAT4

To assess IRF8 regulation in antigen-specific NK cells during MCMV infection, we performed comparative transcriptome analysis by RNA-seq during their adaptive responses. Consistent with a critical role for IRF8 in early viral control by NK cells, *Irf8* was one of the most highly induced transcription factors in activated Ly49H^{+} NK cells (isolated at day 2 p.i.) compared to naïve NK cells (Figure 2A), and was highly expressed and upregulated compared with other IRF family members (Figure 2B). During MCMV infection, IRF8 was upregulated during early NK cell activation at both the transcript and protein levels (Figures 2C and 2D). However, maintenance of maximal IRF8 expression was transient, with both transcript and protein returning nearly to baseline within 1 week and at memory time points (Figures 2C and 2D), suggesting that IRF8 functions in the early programming of antiviral NK cell responses.

IRF8 was first described to be induced in lymphocytes and macrophages by IFN-γ (Driggers et al., 1990); however, IRF8 upregulation in NK cells during MCMV infection was not dependent upon IFN-γ (Figure 3A). Because peak IRF8 expression was observed at early time points *in vivo*, when inflammation is maximal (Biron and Tarrio, 2015), we hypothesized that proinflammatory cytokines such as IL-12, IL-18, or type I interferons may instead be regulating IRF8 induction in activated NK cells. We generated mixed bone marrow chimeric mice, harboring both WT cells and cells deficient in receptors for various proinflammatory cytokines (IL-12, IL-18, or type I interferons) and downstream STAT signaling molecules (STAT1 or STAT4), and challenged them with MCMV (Figure 3B). Compared to WT NK cells, NK cells that were unresponsive to IL-12 signaling (either through absence of the IL-12 receptor or its downstream effector STAT4) were impaired in their ability to maximally upregulate IRF8 after infection (Figure 3C). In contrast, IRF8 upregulation in *Ifnar1*$^{-/-}$, *Il18r1*$^{-/-}$, and *Stat*$^{-/-}$ NK cells remained unaffected (Figure 3C). Collectively, these data suggest an NK cell-specific mechanism of IRF8 regulation by IL-12 and STAT4.

However, IRF8 induction *in vivo* was not fully abrogated in the absence of IL-12 and STAT4 signaling, suggesting a role for other factors. Indeed, Ly49H signaling in NK cells synergized with IL-12 to drive maximal IRF8 induction (Figure 3C), consistent with an analogous report of T cell receptor (TCR) signaling contributing to IRF8 expression in antigen-specific $CD8^+$ T cells (Miyagawa et al., 2012). Furthermore, *ex vivo* stimulation with IL-12 or common γ-chain-dependent cytokines (IL-2, IL-15) was also sufficient to promote IRF8 upregulation in NK cells (Figure S2A). Given the dependence of NK cells on common γ-chain-dependent cytokines for their survival in the periphery (Jamieson et al., 2004; Prlic et al., 2003; Ranson et al., 2003), the contribution of common γ-chain-dependent cytokines in IRF8 induction during MCMV infection *in vivo* cannot be assessed in the same manner as for IL-12. Nevertheless, signaling through these two pathways (Ly49H and common γ-chain-dependent receptors) likely synergized with IL-12 signaling to regulate IRF8 expression in NK cells during MCMV infection.

In agreement with the necessary role for IL-12 and STAT4 signaling in IRF8 induction, STAT4 occupied the *Irf8* promoter by genome-wide chromatin immunoprecipitation coupled to DNA sequencing (ChIP-seq) (Figure 3D), and *Irf8* was among the top ten STAT4-bound transcription factor loci in activated NK cells (Figure S2B). STAT4 binding co-localized with a region of increased accessibility in the *Irf8* promoter in $Ly49H^+$ NK cells at day 2 p.i., revealed by an assay for transposase-accessible chromatin with high throughput sequencing (ATAC-seq) (Figures 3D and S2C). Furthermore, we detected STAT4-dependent trimethylation of histone H3 at lysine 4 (H3K4me3, which marks transcriptionally active promoters) at the *Irf8* locus in NK cells stimulated with proinflammatory cytokines (Figure 3E). Together, these data suggest that STAT4 may be actively remodeling the epigenetic landscape to promote IRF8 induction in activated NK cells. Given the requirement for IL-12 and STAT4 for the clonal expansion of effector NK cells and the generation of memory NK cells (Sun et al., 2012), IRF8 appears to represent a key effector molecule downstream of the IL-12 and STAT4 axis driving a transcriptional program that supports antiviral NK cell responses.

NK cells require IRF8 for virus-driven expansion

MCMV-induced NK cell activation results in rapid production and release of cytolytic molecules (e.g. perforin, granzyme B) and proinflammatory cytokines (e.g. IFN-γ), resulting in lysis of infected cells and establishment of an antiviral state, as well as antigen-specific clonal proliferation of the $Ly49H^+$ NK cell subset (Sun and Lanier, 2011). Given the poor protective capacity of NK-$Irf8^{-/-}$ NK cells, we sought to delineate which of these effector functions was regulated by IRF8. WT and NK-$Irf8^{-/-}$ NK cells demonstrate comparable proinflammatory cytokine-dependent activation and IFN-γ production during MCMV infection *in vivo* (Figures S3A and S3B), as well as following cytokine, or PMA and ionomycin stimulation *in vitro* (Figure S3C). Compared to WT cells, granzyme B production was similarly unaffected in NK-$Irf8^{-/-}$ NK cells (Figure S3B), resulting in normal *in vivo* elimination of m157-expressing target cells (Figure S3D).

To test the role for IRF8 in MCMV-driven NK cell expansion, we adoptively co-transferred WT and NK-$Irf8^{-/-}$ NK cells at equal numbers into Ly49H-deficient recipient mice

(*Klra8*$^{-/-}$), infected the recipients with MCMV, and tracked the transferred effector Ly49H^{+} NK cell response in the recipients (Figure 4A). In contrast to WT NK cells, which expanded robustly and reached peak numbers at day 7 p.i., NK-*Irf8*$^{-/-}$ NK cells were significantly reduced at this time point (Figure 4B). However, NK cells from Cre-negative littermate control mice expanded comparably to WT cells (Figure S3E). The defective expansion of NK-*Irf8*$^{-/-}$ NK cells was observed as early as day 3 p.i., and was consistent across various organs (Figure 4C), excluding impaired trafficking as an explanation for the observed phenotype. However, despite the poor expansion, IRF8 deficiency did not impair the terminal maturation of NK cells during infection (Figures S3F and S3G).

Furthermore, a severely diminished pool of NK-*Irf8*$^{-/-}$ memory NK cells was observed at day 30 p.i. compared to WT memory NK cells (Figures 4B and 4D). Although reduced in number, IRF8-deficient memory NK cells were functional upon re-stimulation (Figure S3H). To determine whether IRF8 was required for adaptive NK cell responses against other viruses, we infected mice with recombinant vesicular stomatitis virus engineered to express the MCMV *m157* gene (VSV-*m157*). During VSV-*m157* infection, NK-*Irf8*$^{-/-}$ NK cells were similarly outcompeted by WT NK cells, and ultimately formed a smaller pool of memory NK cells (Figure 4E), suggesting that the requirement for IRF8 in antigen-specific NK cell expansion is not limited to MCMV infection. However, IRF8 was not required for hapten-specific NK cell-mediated contact hypersensitivity responses (Figure S4), suggesting IRF8 only plays a critical role during infectious priming, but not non-infectious priming, of adaptive NK cell responses.

To address whether IRF8 directly maintained virus-specific memory NK cell numbers, we generated a mouse model in which the floxed exon 2 of *Irf8* can be excised by a tamoxifen-inducible Cre cassette driven by the ubiquitin promoter (*Ubc*$^{Cre\text{-}ERT2}$ *Irf8*$^{fl/fl}$). In our adoptive co-transfer system, recipient mice were treated with either tamoxifen or oil just prior to the contraction phase (treatment days 7–9 p.i.), resulting in successful deletion of *Irf8* in tamoxifen-, but not oil-treated, *Ubc*$^{Cre\text{-}ERT2}$ *Irf8*$^{fl/fl}$ NK cells (Figure S3I). Inducible deletion of *Irf8* after NK cell expansion did not affect formation of the memory NK cell pool, as *Ubc*$^{Cre\text{-}ERT2}$ *Irf8*$^{fl/fl}$ memory NK cells were found at similar proportions in the blood of tamoxifen- and oil-treated mice (Figure S3I). Thus, IRF8 is essential in driving the expansion, but not the memory maintenance of virus-specific NK cells.

NK cells also undergo homeostatic proliferation in a lymphopenic environment, thought to be driven by availability of common γ-chain-dependent cytokines (Sun et al., 2011). NK-*Irf8*$^{-/-}$ NK cells were found to be defective in homeostatic proliferation following adoptive transfer into *Rag2*$^{-/-}$ *IL2rg*$^{-/-}$ mice, which lack both innate and adaptive lymphocytes (Figure S5A). Consistent with common γ-chain-dependent IRF8 expression in CD8^{+} T cells (Miyagawa et al., 2012) and human NK cells (Mace et al., 2017), IRF8 abundance trended upwards in lymphopenia-driven NK cells (Figure S5B). These findings collectively indicate that IRF8 is specifically required to support robust expansion of mature NK cell numbers during infection and homeostatic proliferation, whereas redundant mechanisms exist for NK cell development or homeostatic maintenance, which necessitate modest cell turnover.

IRF8 promotes proliferation through direct regulation of *Zbtb32*

To investigate pathways regulated by IRF8 that may be promoting NK cell expansion, we performed comparative transcriptome analysis by RNA-seq on purified WT and NK-*Irf8*$^{-/-}$ NK cells derived from MCMV-infected and -uninfected mixed bone marrow chimeric mice (Figure 5A). Consistent with the reported ability of IRF8 to act as a transcriptional activator or repressor depending on its binding partner (Tamura et al., 2015), 323 transcripts were downregulated, and 379 transcripts were upregulated in NK-*Irf8*$^{-/-}$ NK cells at day 4 p.i. compared to WT NK cells (Table S1). Classification of differentially expressed genes into PANTHER pathways revealed a transcriptional program consistent with dysregulated cell cycle control, DNA replication, and metabolism in NK-*Irf8*$^{-/-}$ NK cells (Figure S6A). Because these gene sets trended towards being comparatively enriched in WT NK cells (Figure 5B), we tested whether cell proliferation was defective in NK-*Irf8*$^{-/-}$ NK cells. Indeed, analysis of WT and NK-*Irf8*$^{-/-}$ NK cells labeled with Cell Trace Violet (CTV) prior to adoptive co-transfer and MCMV infection confirmed that NK-*Irf8*$^{-/-}$ NK cells fail to divide efficiently (Figure 5C). In contrast, NK-*Irf8*$^{-/-}$ NK cells exhibited no evidence of enhanced caspase activation, and normal expression of the pro-survival protein Bcl-2 during MCMV-driven expansion (Figures S6B and S6C). Collectively, these data indicate that IRF8 is essential for inducing a broad transcriptional program that primarily serves to promote MCMV-driven NK cell proliferation.

We next sought to pinpoint key transcriptional targets of IRF8 that promote NK cell proliferation during infection *in vivo*. Given that there exist baseline transcriptional differences between WT and NK-*Irf8*$^{-/-}$ NK cells (Figure 5A), yet no NK cell developmental phenotype in the absence of IRF8 (Figure S1), we reasoned that infection-specific transcriptional differences would likely best explain the impaired proliferation of NK-*Irf8*$^{-/-}$ NK cells. Our RNA-seq analysis identified a subset of genes that were differentially upregulated or downregulated in NK-*Irf8*$^{-/-}$ NK cells in an infection-specific manner (Figures 6A, 6B, and S6D). One such gene was *Zbtb32*, which was more highly induced in WT than in NK-*Irf8*$^{-/-}$ NK cells during MCMV infection (Figures 6A-6C). Zbtb32 is a Broad complex, Tramtrack, Bric á Brac and Zinc Finger (BTB-ZF) transcription factor previously reported to be essential for the proliferative burst of MCMV-specific NK cells (Beaulieu et al., 2014). *In silico* analysis identified multiple IRF8 binding sites that fall in moderate-to-highly conserved non-coding sequence (CNS) regions within the *Zbtb32* locus (Figure 6D), some of which are bound by IRF8 in other immune cells (Langlais et al., 2016; Marquis et al., 2011; Shin et al., 2011). Moreover, IRF8 ChIP followed by qPCR revealed enrichment of *Zbtb32* promoter DNA (compared to gene desert following immunoprecipitation with α-IRF8 antibody), confirming that *Zbtb32* is a direct target of IRF8-mediated transcriptional activation (Figure 6E). However, during MCMV infection, IRF8 induction in NK cells was found to be independent of Zbtb32 (Figure S6E). Given that the *Zbtb32* locus is IRF8-bound (Figure 6E) and that *Zbtb32* expression is IRF8-dependent (Figures 6A-6C), we thus propose a model wherein IRF8 functions upstream of Zbtb32 to drive antiviral NK cell proliferation.

Discussion

A growing body of literature supports the paradigm that NK cells in mice, primates, and humans undergo antigen-specific responses to viral pathogens (Adams et al., 2016). Adaptive NK cell responses include the prolific expansion and memory formation of virus-specific NK cell subsets (Sun et al., 2009), yet the transcriptional control of these processes is poorly understood. Here, we have revealed that the transcription factor IRF8 is dynamically regulated in antigen-specific NK cells during viral infection and is essential for NK cell-mediated immunity against MCMV. In contrast to its canonical regulation throughout the immune system by IFN-γ (Driggers et al., 1990), we herein describe that the proinflammatory cytokine IL-12 and the activating receptor Ly49H represent the critical signals for maximal IRF8 upregulation in NK cells early during MCMV infection. Given that IL-12, but not IFN-γ, is required for MCMV-driven NK cell expansion (Sun et al., 2012), IL-12-dependent regulation uniquely positions IRF8 to exert a functional role over antiviral NK cell responses.

Notably, *Irf8*$^{-/-}$ mice have greater viral susceptibility than do NK-*Irf8*$^{-/-}$ mice. Several studies have delineated a role for IRF8 in the development of monocytes, pDCs, and cDC1s, which are all affected in *Irf8*$^{-/-}$ mice (Aliberti et al., 2003; Schiavoni et al., 2002). Loss of IRF8-dependent CD8α^{+} cDC1s in *Irf8*$^{-/-}$ mice has been demonstrated to impair IL-12 production in a variety of pathogen models (Giese et al., 1997; Scharton-Kersten et al., 1997). During early MCMV infection, IRF8-dependent cDC1s are the major producer of IL-12 (Weizman et al., 2017), and IL-12 signaling is critical for programming adaptive NK cell responses to MCMV infection (Sun et al., 2012). Thus, the striking mortality of *Irf8*$^{-/-}$ mice during MCMV infection is likely a combination of both cell-extrinsic (impaired NK cell priming due to low systemic IL-12 in the absence of cDC1s) and cell-intrinsic (impaired IRF8-dependent NK cell proliferative burst) functions for IRF8.

During MCMV infection, we observed that IRF8 drives a transcriptional program consistent with cell cycle progression, which supports NK cell clonal proliferation such that NK cells can mount a maximal effector response. Our data suggest that the output of the IRF8 transcriptional program is likely mediated in part by IRF8 directly binding to the *Zbtb32* locus to promote expression of Zbtb32, a pro-proliferative transcription factor previously reported to be essential for controlling the proliferative burst of virus-specific NK cells (Beaulieu et al., 2014), thus elucidating a previously uncharacterized relationship between these two transcription factors. Given its function, Zbtb32 is tightly regulated by NK cells during both homeostasis and MCMV infection. Naïve NK cells do not express Zbtb32, but NK cells transiently upregulate *Zbtb32* nearly 100-fold during MCMV infection in a manner similarly dependent on IL-12 signaling (Beaulieu et al., 2014). Maximal Zbtb32 induction is critical, as *Zbtb32* hemizygosity is insufficient to drive NK cell expansion during viral infection (Beaulieu et al., 2014). Because STAT4 itself also directly regulates *Zbtb32* expression, this may explain why only an incomplete, yet not abrogated, *Zbtb32* upregulation was observed in the absence of IRF8. Because additional transcription factors may also be regulating *Zbtb32* transcription (either individually or in concert with STAT4 and IRF8), it will be important to determine the complete mechanisms that ensure a robust IL-12 and STAT4 effector program within activated NK cells.

Despite the requirement for IRF8 in NK cell antiviral immunity, we observed no impact of IRF8 deficiency on NK cell development. This observation appears inconsistent with findings in patients with biallelic *IRF8* mutations across 3 unrelated families who exhibit impaired terminal maturation and diminished overall numbers of NK cells (Mace et al., 2017). Perhaps this discrepancy can be ascribed to our use of a specific deletion of *Irf8* in NK cells of transgenic mice, whereas NK cells in these patients developed in the presence of hematopoietic and stromal cells that also bear the *IRF8* mutations. Despite carrying biallelic *IRF8* mutations, the NK cell deficient patient had normal amounts of IRF8 protein, which translocated normally to the nucleus and demonstrated unaffected transcriptional activity dependent on PU.1 and IRF1, two of its canonical binding partners (Mace et al., 2017). Thus, the mutant IRF8 protein in humans may have adopted an altered function within the NK cell population rather than representing a nonfunctional protein or the ablated gene we investigated in mice.

In our study, we have delineated a dichotomous requirement for IRF8 in NK cells that appears to be dependent on the degree of cell turnover, as IRF8 was required for MCMV- and lymphopenia-driven proliferation, but dispensable for development and homeostatic maintenance. However, it remains unclear how IRF8 is targeted for transcriptional activity during different cellular states. Recent studies have found that dynamic epigenetic changes accompany $CD8^+$ T cell differentiation during bacterial and viral infection, and can modulate the availability of transcription factor binding sites (Pauken et al., 2016; Russ et al., 2014; Scharer et al., 2013; Scott-Browne et al., 2016; Sen et al., 2016; Yu et al., 2017). Furthermore, due to structural divergences in its IRF domain (Escalante et al., 2002), IRF8 requires a DNA-binding partner (e.g. Ets, AP-1, or other IRF family members) to bind DNA with high affinity (Tamura et al., 2008). It is unknown whether IRF8 utilizes the same binding partners in NK cells as it does in other hematopoietic cells, yet the availability or modification of binding partners secondary to different NK cell states may dictate the set of genes regulated by IRF8. Indeed, this mechanism has been described in macrophages wherein the ability of IRF8 to bind alternative DNA sequences after LPS or IFN-γ stimulation is dependent on stimulus-inducible partners (Kuwata et al., 2002; Mancino et al., 2015). Further understanding of the complete molecular mechanisms that regulate IRF8 transcriptional activity will offer valuable insights into how antigen-specific NK cells generate robust proliferative responses to viral infection.

In summary, our work highlights the importance of IRF8 in orchestrating adaptive NK cell antiviral responses. Because proinflammatory cytokines are necessary and sufficient for IRF8 upregulation in NK cells, it will be of interest to test whether IRF8 is similarly induced and required for the function of other innate lymphoid cell (ILC) lineages, which lack antigen receptors and are thought to initiate antimicrobial responses by sensing cytokines, alarmins, and inflammatory mediators (Sonnenberg and Artis, 2015). Analogous to expansion of mouse $Ly49H^+$ NK cells during MCMV infection, HCMV-seropositive individuals exhibit an expanded and long-lived population of $NKG2C^+$ NK cells (Gumá et al., 2004; Hendricks et al., 2014; Lopez-Vergès et al., 2011) that are capable of recall responses (Foley et al., 2012). Whether these adaptive NK cell responses in humans similarly require IRF8 during HCMV infection remains to be determined. Nevertheless, our results uncover molecular events that provide insight into the upstream regulation and

downstream transcriptional program of IRF8, and shed light on ways to modulate NK cell antiviral immunity for therapeutic benefit.

STAR Methods

Contact for Reagent and Resource Sharing

Further information and requests for resources and reagents should be directed to and will be fulfilled by the Lead Contact, Joseph Sun (sunj@mskcc.org).

Experimental Model and Subject Details

Mice—All mice used in this study were housed and bred under specific pathogen-free conditions at Memorial Sloan Kettering Cancer Center, and handled in accordance with the guidelines of the Institutional Animal Care and Use Committee (IACUC). The following mouse strains were used in this study: C57BL/6 (CD45.2), B6.SJL (CD45.1), B6 CD45.1×CD45.2, *Irf8*$^{-/-}$, *Irf8*$^{fl/fl}$, *Nkp46*^{iCre} (Narni-Mancinelli et al., 2011), *Nkp46*^{iCre} *Irf8*$^{fl/fl}$, *Ubc*$^{Cre\text{-}ERT2}$, *Ubc*$^{Cre\text{-}ERT2}$ *Irf8*$^{fl/fl}$, *Klra8*$^{-/-}$ (Ly49H-deficient) (Fodil-Cornu et al., 2008), *Ifngr1*$^{-/-}$, *Il12rb2*$^{-/-}$, *Stat4*$^{-/-}$, *Ifnar1*$^{-/-}$, *Stat1*$^{-/-}$, *Il18r1*$^{-/-}$, m157-Tg (Tripathy et al., 2008), *Rag2*$^{-/-}$ *IL2rg*$^{-/-}$, and *Zbtb32*$^{-/-}$ (Hirahara et al., 2008). Experiments were conducted using age- and gender-matched mice in accordance with approved institutional protocols.

Virus—MCMV (Smith strain) was serially passaged through BALB/c hosts three times, and then salivary gland viral stocks were prepared with a dounce homogenizer for dissociating the salivary glands of infected mice 3 weeks after infection. Recombinant VSV-*m157* was made by cloning the coding sequence for the MCMV glycoprotein m157 into the parental VSV Indiana strain provided by K. Schluns (MD Anderson) (Firth et al., 2013).

Method Details

Mixed Bone Marrow Chimeras—Mixed bone marrow chimeric mice were generated by lethally irradiating (900 cGy) host CD45.1×CD45.2 animals and reconstituting them with a 1:1 mixture of bone marrow cells from WT (CD45.1) and genetic-deficient (CD45.2) donor mice. Hosts were co-injected with anti-NK1.1 (clone PK136) to deplete any residual donor or host mature NK cells. CD45.1^{+}CD45.2^{+} host NK cells were excluded from all analyses.

***In vivo* Virus Infection—**Adoptive co-transfer studies were performed by transferring splenocytes from WT (CD45.1) and genetic-deficient (CD45.2) mice, mixed to achieve equal numbers of Ly49H^{+} KLRG1^{lo} NK cells, into *Klra8*$^{-/-}$ recipients 1 day prior to MCMV infection. Recipient mice in adoptive co-transfer studies were infected either with MCMV by i.p. injection of 7.5×10^2 plaque-forming units (PFU) in 0.5 mL or with VSV-*m157* by i.v. injection of 1×10^7 PFU in 0.2 mL. Mixed bone marrow chimeric mice and mice in survival experiments received 7.5×10^3 PFU or 4×10^4 PFU MCMV respectively in 0.5 mL by i.p. injection.

In some experiments, recipient mice were treated for 3 consecutive days with 4 mg/day of tamoxifen (Sigma) dissolved in 0.2 mL corn oil or with 0.2 mL corn oil control (Sigma) by oral gavage, beginning on day 7 after infection.

Hapten Contact Hypersensitivity—To study NK cell-mediated contact hypersensitivity responses, experimental mice were depleted of circulating T cells with 100 μg anti-CD8α (Bio X Cell, clone 2.43) and 400 μg anti-CD4 (Bio X Cell, clone GK1.5) depletion antibodies 3 days prior to sensitization as well as on the days of sensitization and challenge. Mice were sensitized on consecutive days by treating the shaved abdominal skin with 20 μL of 0.5% 1-fluoro-2,4-dinitrobenzene (DNFB, Sigma) in a 4:1 mixture of acetone (Fisher Scientific) to olive oil (Sigma). Mice were challenged 4 days later by treating both surfaces of the left ear with 10 μL of 0.45% DNFB in a 4:1 acetone to olive oil mixture. Both surfaces of the contralateral ear were treated with 10 μL of a 4:1 acetone to olive oil mixture (vehicle) as a control. Ear thickness was measured using a Käfer dial thickness gauge (Long Island Indicator Service).

Virus Quantification—MCMV viral titers were determined as previously described (Johnson et al., 2016). DNA was isolated from peripheral blood using the QIAamp DNA Blood Mini Kit (Qiagen). Following isolation, the DNA concentration was measured using Nanodrop for each sample, and 3 μL was added into a mastermix containing iQ SYBR Green (Bio-Rad) and primers specific to MCMV IE-1 DNA (forward: TCGCCCATCGTTTCGAGA, reverse: TCTCGTAGGTCCACTGACGGA). Copy number was determined by comparing Cq values to a standard curve of known dilutions of an MCMV plasmid and normalizing relative to total DNA content.

Lymphocyte Isolation—Spleens were dissociated using glass slides and filtered through a 100-μm strainer. To isolate lymphocytes from liver, the tissue was physically dissociated using a glass tissue homogenizer and purified using a discontinuous gradient of 40% over 60% Percoll. To isolate cells from the lung, the tissue was physically dissociated using scissors and incubated for 30 minutes in digest solution (1 mg/mL type D collagenase in RPMI supplemented with 5% fetal calf serum, 1% L-glutamine, 1% penicillin-streptomycin, and 10 mM HEPES). Resulting dissociated tissue was passed through 100-μm strainers, centrifuged, and lymphocytes were removed from the supernatant. To isolate bone marrow lymphocytes, cleaned femur and tibia bones were ground with mortar and pestle, and the resulting solution filtered through a 100-μm strainer. Red blood cells in spleen, liver, lung, and bone marrow were lysed using ACK lysis buffer.

Flow Cytometry and Cell Sorting—Cell surface staining of single-cell suspensions from various organs was performed using fluorophore-conjugated antibodies (BD Biosciences, eBioscience, BioLegend, Tonbo Biosciences, Cell Signaling Technology). Intracellular staining was performed by fixing and permeabilizing with the eBioscience Foxp3 Transcription Factor Staining Set (Thermo Fisher) for staining intranuclear proteins and cytokines, or with formaldehyde and methanol for staining phosphorylated STAT proteins.

Flow cytometry and cell sorting were performed on the LSR II and Aria II cytometers (BD Biosciences), respectively. Data were analyzed with FlowJo software (Tree Star). Flow cytometry of lymphocytes was performed using the following fluorophore-conjugated antibodies: CD3ε (17A2), TCRβ (H57–597), CD19 (6D5), F4/80 (BM8.1), NK1.1 (PK136), NKp46 (29A1.4), Ly49H (3D10), CD45.1 (A20), CD45.2 (104), CD45 (30-F11),

IRF8 (V3GYWCH), CD11b (M1/70), CD27 (LG.7F9), KLRG1 (2F1), Ly49D (4E5), Ly49A (YE1/48.10.6), Ly49C/I (5E6), STAT4 pY693 (38/p-Stat4), STAT5 pY694 (C11C5), F(ab')2 Rabbit IgG (polyclonal), CD69 (H1.2F3), Granzyme B (GB11), IFN-γ (XMG1.2), CD107a (1D4B), CD8α (53–6.7), and Bcl-2 (3F11).

Apoptosis was evaluated by caspase activity staining using the carboxyfluorescein FLICA poly caspase assay kit (Bio-Rad). NK cell proliferation was analyzed by labeling cells with 5 μM CellTrace Violet (CTV, Thermo Fisher) prior to transfer, and CTV labeling was performed according to manufacturer protocol.

***Ex vivo* Stimulation of Lymphocytes—**Approximately 10^6 spleen lymphocytes were stimulated for 4 hours in RPMI containing 10% fetal bovine serum with 20 ng/mL recombinant mouse IL-12 (R&D Systems) plus 10 ng/mL IL-18 (MBL) or 50 ng/mL PMA (Sigma) plus 500 ng/mL Ionomycin (Sigma). Cells were cultured in media alone as a negative control.

Chromatin Immunoprecipitation and Sequencing—5–10 × 10^6 NK cells (TCRβ$^-$CD3ε$^-$CD19$^-$F4/80$^-$NK1.1$^+$) were first enriched from spleens of pooled C57BL/6 mice by negative selection over BioMag goat anti-rat IgG beads (Qiagen) coated with rat anti-mouse CD8α, CD4, CD19, and Ter-119 antibodies (Bio X Cell, clones 2.43, GK1.5, 1D3, and TER-119 respectively), sorted to high purity, and incubated with or without 20 ng/mL IL-12 and 10 ng/mL IL-18 (as well as 10 ng/mL IL-2 and 10 ng/mL IL-15 for IRF8 ChIP, R&D Systems). NK cells were stimulated for 30 min (H3K4me3 ChIP) or 16 hours (STAT4 and IRF8 ChIP). DNA and proteins were cross-linked for 7.5 minutes using 0.75% formaldehyde. ChIP was performed as previously described (Zheng et al., 2007), using 10 μg of rabbit polyclonal anti-STAT4 antibody (Santa Cruz sc-486, clone C-20), 1 μg of rabbit polyclonal anti-trimethyl Histone H3 (Lys4) antibody (H3K4me3, Millipore 07473), or 8 μg of goat polyclonal anti-IRF8 antibody (Santa Cruz sc-6058, clone C-19), followed by qPCR or Illumina next-generation sequencing. qPCR primers for IRF8 ChIP include: *Zbtb32* (forward: TACGGCGATCATCCCTCCTT, reverse: AGAGCATCATCTCCCTAGCG), and gene desert 50kB upstream of *Foxp3* (forward: TAGCCAGAAGCTGGAAAGAAGCCA, reverse: TGATACCCTCCAGGTCCAACCATT). After determining the Ct value, percent input was calculated as $100 \times 2^{(\text{Ct adjusted input} - \text{Ct target})}$, where the Ct^{input} was adjusted from 5% to 100% by subtracting $\log_2 20$ from input Ct values.

RNA Sequencing—RNA was isolated from sorted cell populations using TRIzol (Thermo Fisher) and total RNA was amplified using the SMART-seq V4 Ultra Low Input RNA kit (Clontech). Subsequently, 10 ng of amplified cDNA was used to prepare Illumina HiSeq libraries with the Kapa DNA library preparation chemistry (Kapa Biosystems) using 8 cycles of PCR. Samples were barcoded and run on Hiseq 2500 1T, in a 50bp/50bp paired-end run, using the TruSeq SBS Kit v3 (Illumina).

ATAC Sequencing—ATAC-seq libraries were prepared as previously described (Buenrostro et al., 2013). Briefly, fresh cells were washed in cold PBS and lysed. Transposition occurred at 42°C for 45 minutes. DNA was purified using the MinElute PCR purification kit (Qiagen) and amplified for 5 cycles. Additional PCR cycles were evaluated

by real time PCR. Final product was cleaned by Ampure Beads at a 1.5× ratio. Libraries were sequenced on a Hiseq 2500 1T in a 50bp/50bp paired-end run, using the TruSeq SBS Kit v3 (Illumina).

Quantification and Statistical Analysis

ChIP Sequencing Analysis—Analysis of ChIP-seq data was performed as previously described (Rapp et al., 2017).

RNA and ATAC Sequencing Analysis—For both RNA-seq and ATAC-seq, paired-end reads were trimmed for adaptors and removal of low quality reads using Trimmomatic (v. 0.36) (Bolger et al., 2014). Trimmed reads were mapped to the *Mus musculus* genome (mm10 assembly) using Bowtie2 (v2.2.9) (Langmead and Salzberg, 2012). For RNA-seq, read counts for features exons were generated using the summarizeOverlaps function from the GenomicAlignments package(v1.10.1) (Lawrence et al., 2013). Differential analyses were executed with DESeq2 (v1.14.1) (Love et al., 2014) using the UCSC ensGene model as a reference annotation. Gene tracks were generated by converting BAM files to bigWig files using bedtools2 (v.2.26.0) (Quinlan and Hall, 2010) and UCSC's bedGraphToBigWig (v.4) (Kent et al., 2010) and visualized using the Gviz R package (v.1.18.2) (Hahne and Ivanek, 2016). All tracks show genomic coordinates in megabase pairs on the x-axis and normalized tag counts on the y-axis.

The distribution of read counts across all genes was bimodal. The assumption that this corresponded to "expressed" and "non-expressed" genes was supported by examination of marker genes known to be expressed or not expressed in NK cells. The local minimum between the two peaks was chosen to be the threshold for expression.

Gene set enrichment analysis (GSEA) was performed using the v3.0 software running default parameters (Subramanian et al., 2005) (http://www.broad.mit.edu/gsea/), and with genes from significantly overrepresented PANTHER pathways. GSEA plots were replotted into a vector graphics format using the ReplotGSEA script by Thomas Kuilman (https://github.com/PeeperLab/Rtoolbox/blob/master/R/ReplotGSEA.R).

Plots of fold change vs. fold change (Figures 6A and S6D) were used to identify candidate genes of interest (Figure 6B), with the assumption that genes that are insufficiently upregulated or downregulated in NK-*Irf8*$^{-/-}$ NK cells at D4 may account for the D4-specific phenotype observed, despite there also being baseline transcriptional differences between NK-*Irf8*$^{-/-}$ and WT NK cells (Figure 5A). The first plot (Figure 6A) examined genes differentially expressed (| log2 fold change | ≥ 1) between WT and NK-*Irf8*$^{-/-}$ NK cells at D4 (red or blue-colored genes), then further identified a subset of these DE genes for which the magnitude of the difference between WT and NK-*Irf8*$^{-/-}$ is larger on D4 than at D0 ($D4_{Log2FC[WT/NK\text{-}Irf8^{-/-}]} - D0_{Log2FC[WT/NK\text{-}Irf8^{-/-}]} \geq 1$ or $D4_{Log2FC[WT/NK\text{-}Irf8^{-/-}]} - D0_{Log2FC[WT/NK\text{-}Irf8^{-/-}]} \leq -1$). Similarly, a separate fold change plot (Figure S6D) examined genes that are differentially expressed in WT NK cells on D4 vs. D0, and then honed in on a subset of these genes for which the magnitude of the difference between D4 and D0 is larger in WT than in NK-*Irf8*$^{-/-}$ NK cells ($WT_{Log2FC[D4/D0]} - NK\text{-}Irf8^{-/-}{}_{Log2FC[D4/D0]} \geq 1$ or $WT_{Log2FC[D4/D0]} - NK\text{-}Irf8^{-/-}{}_{Log2FC[D4/D0]} \leq -1$). Genes which satisfied both of these

analyses, and which showed statistical significance ($p_{adj} < 0.05$) in their respective initial differential expression analyses, excluding pseudogenes and genes with ambiguous annotation, are plotted as a heatmap (Figure 6B).

Statistical Analyses—For graphs, data are shown as mean ± SEM, and unless otherwise indicated, statistical differences were evaluated using a two-tailed unpaired Student's t test, assuming equal sample variance. Statistical differences in survival were determined by Gehan-Breslow-Wilcoxon Test analysis. $p < 0.05$ was considered significant. Graphs were produced and statistical analyses were performed using GraphPad Prism.

Data Availability

ChIP-seq, RNA-seq (timecourse), and ATAC-seq datasets are available in the Gene Expression Omnibus (GEO) repository as a SuperSeries under accession code GSE106139. RNA-seq data comparing WT and NK-*Irf8*$^{-/-}$ NK cells before and after MCMV infection are available in GEO under accession code GSE112948.

Supplementary Material

Refer to Web version on PubMed Central for supplementary material.

Acknowledgments

We thank members of the Sun lab for technical support and experimental assistance, and Alexander Rudensky, Ming Li, David Artis, and members of the MSKCC NK club for comments and discussions. Eric Vivier, Toshinori Nakayama, Mark Kaplan, Silvia Vidal, Sandeep Tripathy, and Ken Murphy provided mice critical to this study. N.M.A. and X.F. were supported by an MSTP grant from the NIGMS of the NIH to the Weill Cornell/Rockefeller/Sloan Kettering Tri-Institutional MD-PhD Program (T32GM007739), and an F30 Predoctoral Fellowship from NIAID of the NIH (F30 AI136239–01A1 to N.M.A., F30 AI122721–01 to X.F.) C.M.L. was supported by a T32 award from the NIH (CA009149). M.R. was supported by a fellowship from the DAAD (Germany). J.C.S. was supported by the Ludwig Center for Cancer Immunotherapy, the American Cancer Society, the Burroughs Wellcome Fund, and the NIH (AI100874, AI130043, and P30CA008748).

References

Adams NM, O'Sullivan TE, Geary CD, Karo JM, Amezquita RA, Joshi NS, Kaech SM, and Sun JC (2016). NK cell responses redefine immunological memory. J. Immunol 197, 2963–2970. [PubMed: 27824591]

Aliberti J, Schulz O, Pennington DJ, Tsujimura H, Sousa C.R.e., Ozato K, and Sher A (2003). Essential role for ICSBP in the in vivo development of murine CD8alpha+ dendritic cells. Blood 101, 305–310. [PubMed: 12393690]

Arase H, Mocarski ES, Campbell AE, Hill AB, and Lanier LL (2002). Direct recognition of cytomegalovirus by activating and inhibitory NK cell receptors. Science 296, 1323–1326. [PubMed: 11950999]

Beaulieu AM, Zawislak CL, Nakayama T, and Sun JC (2014). The transcription factor Zbtb32 controls the proliferative burst of virus-specific natural killer cells responding to infection. Nat. Immunol 15, 546–553. [PubMed: 24747678]

Biron CA, Byron KS, and Sullivan JL (1989). Severe herpesvirus infections in an adolescent without natural killer cells. N. Engl. J. Med 29, 1731–1735.

Biron CA, and Tarrio ML (2015). Immunoregulatory cytokine networks: 60 years of learning from murine cytomegalovirus. Med. Microbiol. Immunol 204, 345–354. [PubMed: 25850988]

Bolger AM, Lohse M, and Usadel B (2014). Trimmomatic: a flexible trimmer for Illumina sequence data. Bioinformatics 30, 2114–2120. [PubMed: 24695404]

Buenrostro JD, Giresi PG, Zaba LC, Chang HY, and Greenleaf WJ (2013). Transposition of native chromatin for fast and sensitive epigenomic profiling of open chromatin, DNA-binding proteins and nucleosome position. Nat. Methods 10, 1213–1218. [PubMed: 24097267]

Bukowski JF, Warner JF, Dennert G, and Welsh RM (1985). Adoptive transfer studies demonstrating the antiviral effect of natural killer cells in vivo. J. Exp. Med 161, 40–52. [PubMed: 2981954]

Daniels KA, Devora G, Lai WC, O'Donnell CL, Bennett M, and Welsh RM (2001). Murine cytomegalovirus is regulated by a discrete subset of natural killer cells reactive with monoclonal antibody to Ly49H. J. Exp. Med 194, 29–44. [PubMed: 11435470]

Dokun AO, Kim S, Smith HR, Kang HS, Chu DT, and Yokoyama WM (2001). Specific and nonspecific NK cell activation during virus infection. Nat. Immunol 2, 951–956. [PubMed: 11550009]

Driggers PH, Ennist DL, Gleason SL, Mak WH, Marks MS, Levi BZ, Flanagan JR, Appella E, and Ozato K (1990). An interferon gamma-regulated protein that binds the interferon-inducible enhancer element of major histocompatibility complex class I genes. Proc. Natl. Acad. Sci. USA 87.

Duncan GS, Mittrücker HW, Kägi D, Matsuyama T, and Mak TW (1996). The transcription factor interferon regulatory factor-1 is essential for natural killer cell function in vivo. J. Exp. Med 184, 2043–2048. [PubMed: 8920893]

Escalante CR, Brass AL, Pongubala JM, Shatova E, Shen L, Singh H, and Aggarwal AK (2002). Crystal structure of PU.1/IRF-4/DNA ternary complex. Mol. Cell 10, 1097–1105. [PubMed: 12453417]

Etzioni A, Eidenschenk C, Katz R, Beck R, Casanova JL, and Pollack S (2005). Fatal varicella associated with selective natural killer cell deficiency. J. Pediatr 146, 423–425. [PubMed: 15756234]

Firth MA, Madera S, Beaulieu AM, Gasteiger G, Castillo EF, Schluns KS, Kubo M, Rothman PB, Vivier E, and Sun JC (2013). Nfil3-independent lineage maintenance and antiviral response of natural killer cells. J. Exp. Med 210, 2981–2990. [PubMed: 24277151]

Fodil-Cornu N, Lee SH, Belanger S, Makrigiannis AP, Biron CA, Buller RM, and Vidal SM (2008). Ly49h-deficient C57BL/6 mice: a new mouse cytomegalovirus-susceptible model remains resistant to unrelated pathogens controlled by the NK gene complex. J. Immunol 181, 6394–6405. [PubMed: 18941230]

Foley B, Cooley S, Verneris MR, Curtsinger J, Luo X, Waller EK, Anasetti C, Weisdorf D, and Miller JS (2012). Human cytomegalovirus (CMV)-induced memory-like NKG2C(+) NK cells are transplantable and expand in vivo in response to recipient CMV antigen. J. Immunol 189, 5082–5088. [PubMed: 23077239]

Giese NA, Gabriele L, Doherty TM, Klinman DM, Tadesse-Heath L, Contursi C, Epstein SL, and H.C.M., 3rd (1997). Interferon (IFN) consensus sequence-binding protein, a transcription factor of the IFN regulatory factor family, regulates immune responses in vivo through control of interleukin 12 expression. J. Exp. Med 186, 1535–1546. [PubMed: 9348311]

Gumá M, Angulo A, Vilches C, Gómez-Lozano N, Malats N, and López-Botet M (2004). Imprint of human cytomegalovirus infection on the NK cell receptor repertoire. Blood 104, 3664–3671. [PubMed: 15304389]

Hahne F, and Ivanek R (2016). Visualizing genomic data using Gviz and Bioconductor. Methods Mol. Biol 1418, 335–351. [PubMed: 27008022]

Hendricks DW, Jr HHB, Dunmire SK, Schmeling DO, Hogquist KA, and Lanier LL (2014). Cutting edge: NKG2C(hi)CD57+ NK cells respond specifically to acute infection with cytomegalovirus and not Epstein-Barr virus. J. Immunol 192, 4492–4496. [PubMed: 24740502]

Herzig Y, Nevo S, Bornstein C, Brezis MR, Ben-Hur S, Shkedy A, Eisenberg-Bord M, Levi B, Delacher M, Goldfarb Y, et al. (2017). Transcriptional programs that control expression of the autoimmune regulator gene Aire. Nat. Immunol 18, 161–172. [PubMed: 27941786]

Hirahara K, Yamashita M, Iwamura C, Shinoda K, Hasegawa A, Yoshizawa H, Koseki H, Gejyo F, and Nakayama T (2008). Repressor of GATA regulates TH2-driven allergic airway inflammation and airway hyperresponsiveness. J. Allergy Clin. Immunol 122, 512–520. [PubMed: 18620745]

Holtschke T, Löhler J, Kanno Y, Fehr T, Giese N, Rosenbauer F, Lou J, Knobeloch KP, Gabriele L, Waring JF, et al. (1996). Immunodeficiency and chronic myelogenous leukemia-like syndrome in mice with a targeted mutation of the ICSBP gene. Cell 87, 307–317. [PubMed: 8861914]

Jamieson AM, Isnard P, Dorfman JR, Coles MC, and Raulet DH (2004). Turnover and proliferation of NK cells in steady state and lymphopenic conditions. J. Immunol 172, 864–870. [PubMed: 14707057]

Johnson LR, Weizman OE, Rapp M, Way SS, and Sun JC (2016). Epitope-specific vaccination limits clonal expansion of heterologous naive T cells during viral challenge. Cell Rep. 17, 636–644. [PubMed: 27732841]

Kent WJ, Zweig AS, Barber G, Hinrichs AS, and Karolchik D (2010). BigWig and BigBed: enabling browsing of large distributed datasets. Bioinformatics 26, 2204–2207. [PubMed: 20639541]

Kuwata T, Gongora C, Kanno Y, Sakaguchi K, Tamura T, Kanno T, Basrur V, Martinez R, Appella E, Golub T, and Ozato K (2002). Gamma interferon triggers interaction between ICSBP (IRF-8) and TEL, recruiting the histone deacetylase HDAC3 to the interferon-responsive element. Mol. Cell Biol 22, 7439–7448. [PubMed: 12370291]

Langlais D, Barreiro LB, and Gros P (2016). The macrophage IRF8/IRF1 regulome is required for protection against infections and is associated with chronic inflammation. J. Exp. Med 213, 585–603. [PubMed: 27001747]

Langmead B, and Salzberg SL (2012). Fast gapped-read alignment with Bowtie 2. Nat. Methods 9, 357–359. [PubMed: 22388286]

Lanier LL (2005). NK cell recognition. Annu. Rev. Immunol 23, 225–274. [PubMed: 15771571]

Lawrence M, Huber W, Pagès H, Aboyoun P, Carlson M, Gentleman R, Morgan MT, and Carey VJ (2013). Software for computing and annotating genomic ranges. PLoS Comput. Biol 9, e1003118. [PubMed: 23950696]

Lee CH, Melchers M, Wang H, Torrey TA, Slota R, Qi CF, Kim JY, Lugar P, Kong HJ, Farrington L, et al. (2006). Regulation of the germinal center gene program by interferon (IFN) regulatory factor 8/IFN consensus sequence-binding protein. J. Exp. Med 203, 63–72. [PubMed: 16380510]

Lohoff M, Duncan GS, Ferrick D, Mittrücker HW, Bischof S, Prechtl S, Röllinghoff M, Schmitt E, Pahl A, and Mak TW (2000). Deficiency in the transcription factor interferon regulatory factor (IRF)-2 leads to severely compromised development of natural killer and T helper type 1 cells. J. Exp. Med 192, 325–336. [PubMed: 10934221]

Lopez-Vergès S, Milush JM, Schwartz BS, Pando MJ, Jarjoura J, York VA, Houchins JP, Miller S, Kang SM, Norris PJ, et al. (2011). Expansion of a unique $CD57^{+}$ NKG2Chi natural killer cell subset during acute human cytomegalovirus infection. Proc. Natl. Acad. Sci. USA 108, 14725–14732. [PubMed: 21825173]

Love MI, Huber W, and Anders S (2014). Moderated estimation of fold change and dispersion for RNA-seq data with DESeq2. Genome Biol. 15, 550. [PubMed: 25516281]

Lu R, Medina KL, Lancki DW, and Singh H (2003). IRF-4,8 orchestrate the pre-B-to-B transition in lymphocyte development. Genes Dev. 17, 1703–1708. [PubMed: 12832394]

Mace EM, Bigley V, Gunesch JT, Chinn IK, Angelo LS, Care MA, Maisuria S, Keller MD, Togi S, Watkin LB, et al. (2017). Biallelic mutations in IRF8 impair human NK cell maturation and function. J. Clin. Invest 127, 306–320. [PubMed: 27893462]

Madera S, Rapp M, Firth MA, Beilke JN, Lanier LL, and Sun JC (2016). Type I IFN promotes NK cell expansion during viral infection by protecting NK cells against fratricide. J. Exp. Med 213, 225–233. [PubMed: 26755706]

Madera S, and Sun JC (2015). Cutting edge: stage-specific requirement of IL-18 for antiviral NK cell expansion. J. Immunol 194, 1408–1412. [PubMed: 25589075]

Mancino A, Termanini A, Barozzi I, Ghisletti S, Ostuni R, Prosperini E, Ozato K, and Natoli G (2015). A dual cis-regulatory code links IRF8 to constitutive and inducible gene expression in macrophages. Genes Dev. 29, 394–408. [PubMed: 25637355]

Marquis JF, Kapoustina O, Langlais D, Ruddy R, Dufour CR, Kim BH, MacMicking JD, Giguère V, and Gros P (2011). Interferon regulatory factor 8 regulates pathways for antigen presentation in myeloid cells and during tuberculosis. PLoS Genet. 7, e1002097. [PubMed: 21731497]

Miyagawa F, Zhang H, Terunuma A, Ozato K, Tagaya Y, and Katz SI (2012). Interferon regulatory factor 8 integrates T-cell receptor and cytokine-signaling pathways and drives effector differentiation of CD8 T cells. Proc. Natl. Acad. Sci. USA 109, 12123–12128. [PubMed: 22783014]

Narni-Mancinelli E, Chaix J, Fenis A, Kerdiles YM, Yessaad N, Reynders A, Gregoire C, Luche H, Ugolini S, Tomasello E, et al. (2011). Fate mapping analysis of lymphoid cells expressing the NKp46 cell surface receptor. Proc. Natl. Acad. Sci. USA 108, 18324–18329. [PubMed: 22021440]

Ogasawara K, Hida S, Azimi N, Tagaya Y, Sato T, Yokochi-Fukuda T, Waldmann TA, Taniguchi T, and Taki S (1998). Requirement for IRF-1 in the microenvironment supporting development of natural killer cells. Nature 391, 700–703. [PubMed: 9490414]

Pauken KE, Sammons MA, Odorizzi PM, Manne S, Godec J, Khan O, Drake AM, Chen Z, Sen DR, Kurachi M, et al. (2016). Epigenetic stability of exhausted T cells limits durability of reinvigoration by PD-1 blockade. Science 354, 1160–1165. [PubMed: 27789795]

Prlic M, Blazar BR, Farrar MA, and Jameson SC (2003). In vivo survival and homeostatic proliferation of natural killer cells. J. Exp. Med 197, 967–976. [PubMed: 12695488]

Quinlan AR, and Hall IM (2010). BEDTools: a flexible suite of utilities for comparing genomic features. Bioinformatics 26, 841–842. [PubMed: 20110278]

Ranson T, Vosshenrich CA, Corcuff E, Richard O, Müller W, and Santo JPD (2003). IL-15 is an essential mediator of peripheral NK-cell homeostasis. Blood 101, 4887–4893. [PubMed: 12586624]

Rapp M, Lau CM, Adams NM, Weizman OE, O'Sullivan TE, Geary CD, and Sun JC (2017). Core-binding factor β and Runx transcription factors promote adaptive natural killer cell responses. Sci. Immunol 2.

Russ BE, Olshanksy M, Smallwood HS, Li J, Denton AE, Prier JE, Stock AT, Croom HA, Cullen JG, Nguyen ML, et al. (2014). Distinct epigenetic signatures delineate transcriptional programs during virus-specific CD8(+) T cell differentiation. Immunity 41, 853–865. [PubMed: 25517617]

Scharer CD, Barwick BG, Youngblood BA, Ahmed R, and Boss JM (2013). Global DNA methylation remodeling accompanies CD8 T cell effector function. J. Immunol 191, 3419–3429. [PubMed: 23956425]

Scharton-Kersten T, Contursi C, Masumi A, Sher A, and Ozato K (1997). Interferon consensus sequence binding protein-deficient mice display impaired resistance to intracellular infection due to a primary defect in interleukin 12 p40 induction. J. Exp. Med 186, 1523–1534. [PubMed: 9348310]

Schiavoni G, Mattei F, Sestili P, Borghi P, Venditti M, 3rd, H.C.M., Belardelli F, and Gabriele L (2002). ICSBP is essential for the development of mouse type I interferon-producing cells and for the generation and activation of CD8alpha(+) dendritic cells. J. Exp. Med 196, 1415–1425. [PubMed: 12461077]

Scott-Browne JP, López-Moyado IF, Trifari S, Wong V, Chavez L, Rao A, and Pereira RM (2016). Dynamic changes in chromatin accessibility occur in CD8+ T cells responding to viral infection. Immunity 45, 1327–1340. [PubMed: 27939672]

Sen DR, Kaminski J, Barnitz RA, Kurachi M, Gerdemann U, Yates KB, Tsao HW, Godec J, LaFleur MW, Brown FD, et al. (2016). The epigenetic landscape of T cell exhaustion. Science 354, 1165–1169. [PubMed: 27789799]

Shin DM, Lee CH, and H.C.M., 3rd (2011). IRF8 governs expression of genes involved in innate and adaptive immunity in human and mouse germinal center B cells. PLoS One 6, e27384. [PubMed: 22096565]

Sonnenberg GF, and Artis D (2015). Innate lymphoid cells in the initiation, regulation and resolution of inflammation. Nat. Med 21, 698–708. [PubMed: 26121198]

Subramanian A, Tamayo P, Mootha VK, Mukherjee S, Ebert BL, Gillette MA, Paulovich A, Pomeroy SL, Golub TR, Lander ES, and Mesirov JP (2005). Gene set enrichment analysis: a knowledge-based approach for interpreting genome-wide expression profiles. Proc. Natl. Acad. Sci. USA 102, 15545–15550. [PubMed: 16199517]

Sun JC, Beilke JN, Bezman NA, and Lanier LL (2011). Homeostatic proliferation generates long-lived natural killer cells that respond against viral infection. J. Exp. Med 208, 357–368. [PubMed: 21262959]

Sun JC, Beilke JN, and Lanier LL (2009). Adaptive immune features of natural killer cells. Nature 457, 557–561. [PubMed: 19136945]

Sun JC, and Lanier LL (2011). NK cell development, homeostasis and function: parallels with $CD8^+$ T cells. Nat. Rev. Immunol 11, 645–657. [PubMed: 21869816]

Sun JC, Madera S, Bezman NA, Beilke JN, Kaplan MH, and Lanier LL (2012). Proinflammatory cytokine signaling required for the generation of natural klller cell memory. J. Exp. Med 209, 947–954. [PubMed: 22493516]

Taki S, Nakajima S, Ichikawa E, Saito T, and Hida S (2005). IFN regulatory factor-2 deficiency revealed a novel checkpoint critical for the generation of peripheral NK cells. J. Immunol 174, 6005–6012. [PubMed: 15879093]

Taki S, Sato T, Ogasawara K, Fukuda T, Sato M, Hida S, Suzuki G, Mitsuyama M, Shin EH, Kojima S, et al. (1997). Multistage regulation of Th1-type immune responses by the transcription factor IRF-1. Immunity 6, 673–679. [PubMed: 9208840]

Tamura T, Kurotaki D, and Koizumi S (2015). Regulation of myelopoiesis by the transcription factor IRF8. Int. J. Hematol 101, 342–351. [PubMed: 25749660]

Tamura T, Nagamura-Inoue T, Shmeltzer Z, Kuwata T, and Ozato K (2000). ICSBP directs bipotential myeloid progenitor cells to differentiate into mature macrophages. Immunity 13, 155–165. [PubMed: 10981959]

Tamura T, Yanai H, Savitsky D, and Taniguchi T (2008). The IRF family transcripiton factors in immunity and oncogenesis. Annu. Rev. Immunol 26, 535–584. [PubMed: 18303999]

Tripathy SK, Keyel PA, Yang L, Pingel JT, Cheng TP, Schneeberger A, and Yokoyama WM (2008). Continuous engagement of a self-specific activation receptor induces NK cell tolerance. J. Exp. Med 205, 1829–1841. [PubMed: 18606857]

Weizman OE, Adams NM, Schuster IS, Krishna C, Pritykin Y, Lau C, Degli-Esposti MA, Leslie CS, Sun JC, and O'Sullivan TE (2017). ILC1 confer early host protection at initial sites of viral infection. 2017 171, 795–808.

Xu H, Chaudhri VK, Wu Z, Biliouris K, Dienger-Stambaugh K, Rochman Y, and Singh H (2015). Regulation of bifurcating B cell trajectories by mutual antagonism between transcription factors IRF4 and IRF8. Nat. Immunol 16, 1274–1281. [PubMed: 26437243]

Yu B, Zhang K, Milner JJ, Toma C, Chen R, Scott-Browne JP, Pereira RM, Crotty S, Chang JT, Pipkin ME, et al. (2017). Epigenetic landscapes reveal transcription factors that regulate CD8+ T cell differentiation. Nat. Immunol 18, 573–582. [PubMed: 28288100]

Zheng Y, Josefowicz SZ, Kas A, Chu TT, Gavin MA, and Rudensky AY (2007). Genome-wide analysis of Foxp3 target genes in developing and mature regulatory T cells. Nature 445, 936–940. [PubMed: 17237761]

Highlights:

- IRF8 is required for NK cell-mediated protection against MCMV
- Rapid NK cell upregulation of IRF8 during MCMV infection is STAT4-dependent
- IRF8 is essential for MCMV-specific NK cell expansion
- IRF8 supports NK cell proliferation by directly regulating *Zbtb32*

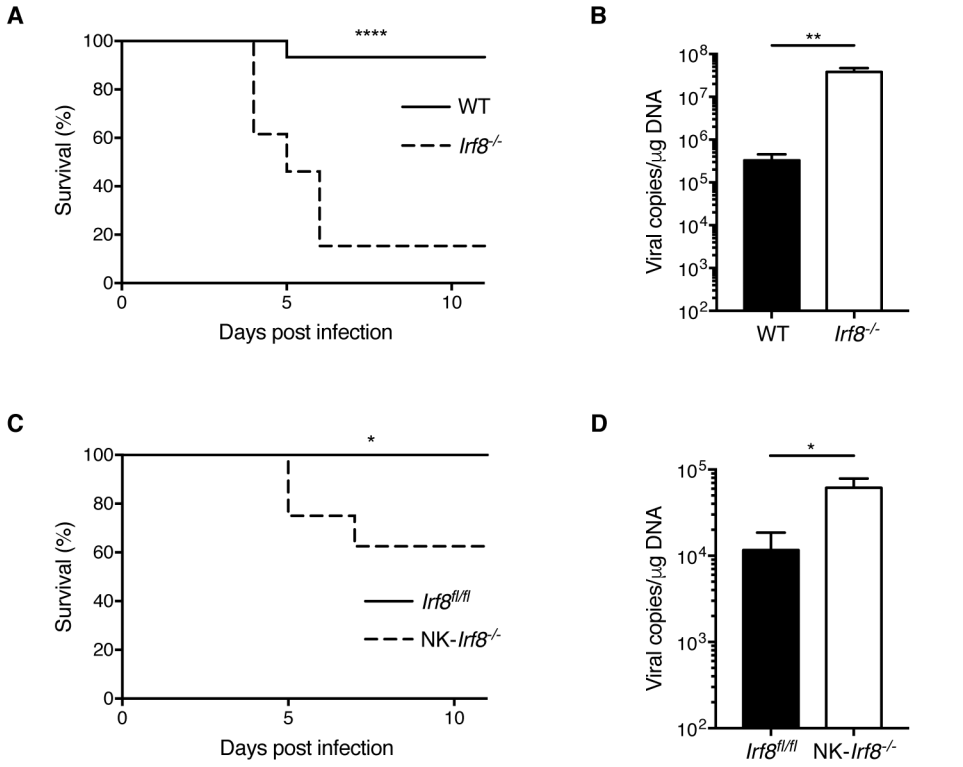

Figure 1. IRF8 is required for NK cell-mediated host protection against MCMV infection

(**A**-**B**) Kaplan-Meier survival curves (A) and peripheral blood viral titers at day 4 p.i. (B) for WT (solid line) and *Irf8*$^{-/-}$ mice (dashed line) challenged intraperitoneally (i.p.) with a lethal dose of MCMV.

(**C**-**D**) Kaplan-Meier survival curves (C) and peripheral blood viral titers at day 4 p.i. (D) for littermate control *Irf8*$^{fl/fl}$ (solid line) and NK-*Irf8*$^{-/-}$ mice (dashed line) challenged i.p. with a lethal dose of MCMV.

Data are representative of three independent experiments with 3–6 mice per group per experiment. Groups were compared using the Gehan-Breslow-Wilcoxon test (A and C), or an unpaired, two-tailed Student's t test (B and D). Data are presented as the mean ± SEM. *$p < 0.05$, **$p < 0.01$, ****$p < 0.0001$). See also Figure S1.

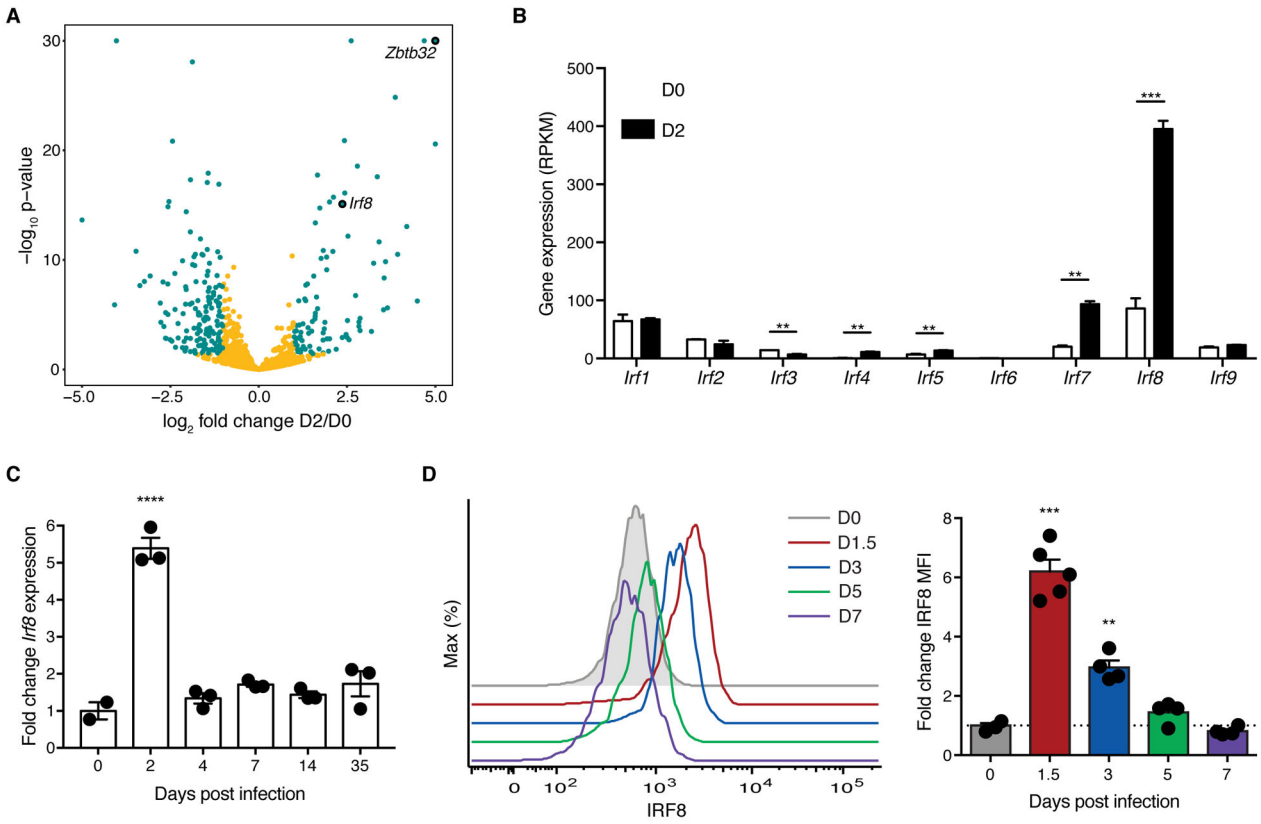

Figure 2. NK cells upregulate IRF8 early during MCMV infection

(**A-C**) Splenocytes were adoptively transferred into Ly49H-deficient mice one day prior to MCMV infection, and Ly49H$^+$ NK cells (TCRβ$^-$CD3$^-$CD19$^-$F4/80$^-$CD45$^+$NK1.1$^+$Ly49H$^+$) were sorted from the spleen at various time points post-infection, followed by RNA-seq (2–3 replicates per time point). (A) Volcano plot comparing expression of loci encoding transcription factors in Ly49H$^+$ NK cells isolated prior to (day 0 p.i.) and following (day 2 p.i.) MCMV infection. Points colored in cyan indicate genes with | Log_2 (D2/D0) | > 1, with $p_{adj} < 0.1$. P values were calculated in DESeq2. (B) RNA-seq reads for IRF family members at day 0 and day 2 p.i. Reads are normalized per exon length and total mapped reads (RPKM). For each gene, time points were compared using an unpaired, two-tailed Student's t test. (C) *Irf8* expression is displayed as the fold change in normalized read number compared with the mean value in NK cells isolated from uninfected mice.

(**D**) Representative flow cytometric histograms of IRF8 expression in splenic Ly49H$^+$ NK cells in MCMV-infected WT mice (left panel). Data is represented as fold change in IRF8 median fluorescence intensity (MFI) in splenic Ly49H$^+$ NK cells at indicated time points following MCMV infection relative to the mean value in uninfected mice (right panel). Data are representative of three independent experiments with 4–5 mice per time point per experiment. Each time point was compared against a hypothetical value of 1 using a one sample t test.

Data are presented as the mean ± SEM. $^{**}p < 0.01$, $^{***}p < 0.001$, $^{****}p < 0.0001$.

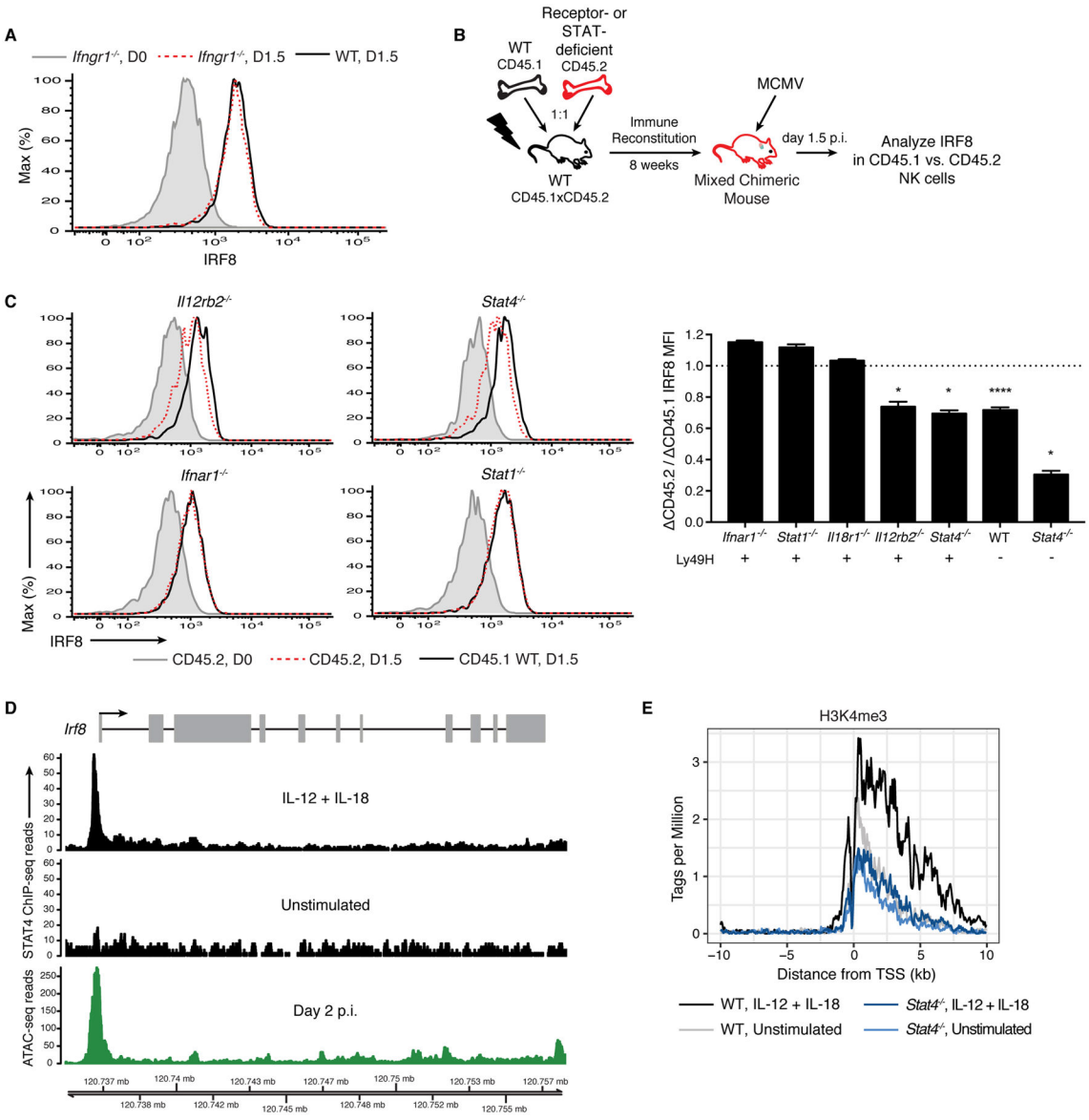

Figure 3. NK cell induction of IRF8 is IL-12 and STAT4-dependent

(**A**) Representative histograms of IRF8 expression in *Ifngr1*$^{-/-}$ NK cells from uninfected (gray line) and infected (red dashed line) chimeric mice, and WT NK cells from infected chimeric mice (black line).

(**B**) Experimental schematic. Mixed bone marrow chimeric mice harboring both WT NK cells (CD45.1) and NK cells deficient in various proinflammatory cytokine receptors and STAT molecules (CD45.2) were infected with MCMV. IRF8 expression in splenic Ly49H^{+} and Ly49H^{-} NK cells was assessed prior to infection and at day 1.5 p.i.

(**C**) Representative histograms of IRF8 expression in various CD45.2 genetically-deficient NK cells from uninfected (gray line) and infected (red dashed line) chimeric mice, and in CD45.1 WT NK cells from infected chimeric mice (black line) (left panels). Data is represented as ΔCD45.2 MFI / ΔCD45.1 WT MFI (Δ = difference in IRF8 MFI between day 0 and 1.5 p.i.) (right panel). Data are representative of two independent experiments with 2–

13 mice per group per time point per experiment. Groups with a ratio < 1 were compared against a hypothetical value of 1 using a one sample t test. Data are presented as the mean ± SEM. *p < 0.05, ****p < 0.0001.

(**D**) Sorted splenic NK cells were stimulated with IL-12 and IL-18 for 16 hours or unstimulated, followed by STAT4 ChIP-seq. STAT4 ChIP-seq reads mapping to the *Irf8* locus are shown in black (top two panels). Data are representative of three independent experiments. Ly49H^{+} NK cells were sorted from the spleen at day 2 p.i, followed by ATAC-seq. ATAC-seq reads mapping to the *Irf8* locus are shown in green (bottom panel). Data are representative of three independent experiments with 2–3 replicates per experiment. *Irf8* exons are shown as gray boxes with black arrow denoting the origin and directionality of transcription.

(**E**) NK cells sorted from spleens of WT or *Stat4*$^{-/-}$ mice were stimulated with IL-12 and IL-18 for 30 min or unstimulated, followed by H3K4me3 ChIP-seq. H3K4me3 signal from *Irf8* locus is plotted as normalized fragment counts binned at 50 bp across a 20-kb window centered on the transcriptional start site (TSS). Data are representative of two independent experiments.

See also Figure S2.

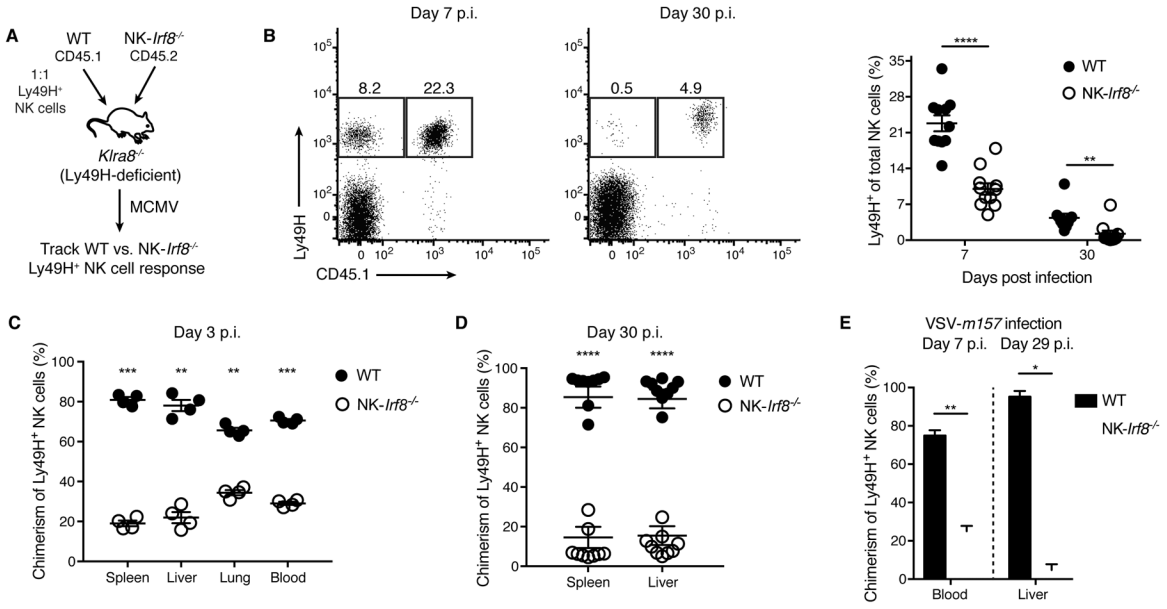

Figure 4. IRF8 is required for NK cell expansion during MCMV infection

(**A**) Experimental schematic. Splenocytes from WT (CD45.1) and NK-*Irf8*$^{-/-}$ mice (CD45.2), mixed to achieve equal numbers of Ly49H^{+} KLRG1^{lo} NK cells, were adoptively co-transferred into *Klra8*$^{-/-}$ recipients 1 day prior to MCMV infection.

(**B**) Representative flow plots gated on NK cells in blood at day 7 p.i. (left) and day 30 p.i. (middle). Quantification of percent WT and NK-*Irf8*$^{-/-}$ Ly49H^{+} NK cells within total NK cells in blood at indicated time points (right).

(**C**) The percentage of WT and NK-*Irf8*$^{-/-}$ NK cells within transferred Ly49H^{+} NK cells in various peripheral organs at day 3 p.i.

(**D**) As in (C), except in spleen and liver at day 30 p.i. Data are representative of two (C) or four (B,D) independent experiments with 4–5 mice per experiment.

(**E**) Experimental design as in (A), except recipient mice were infected with VSV-*m157*. Shown are the percentages of WT and NK-*Irf8*$^{-/-}$ NK cells within transferred Ly49H^{+} NK cells in blood at day 7 p.i. and in liver at day 29 p.i. Data are pooled from two independent experiments.

Groups were compared using an unpaired, two-tailed Student's t test (B) or against a hypothetical value of 50 using a one sample t test (C-E). Data are presented as the mean ± SEM. *p<0.05, **p < 0.01, ***p < 0.001, ****p < 0.0001. See also Figures S3, S4, and S5.

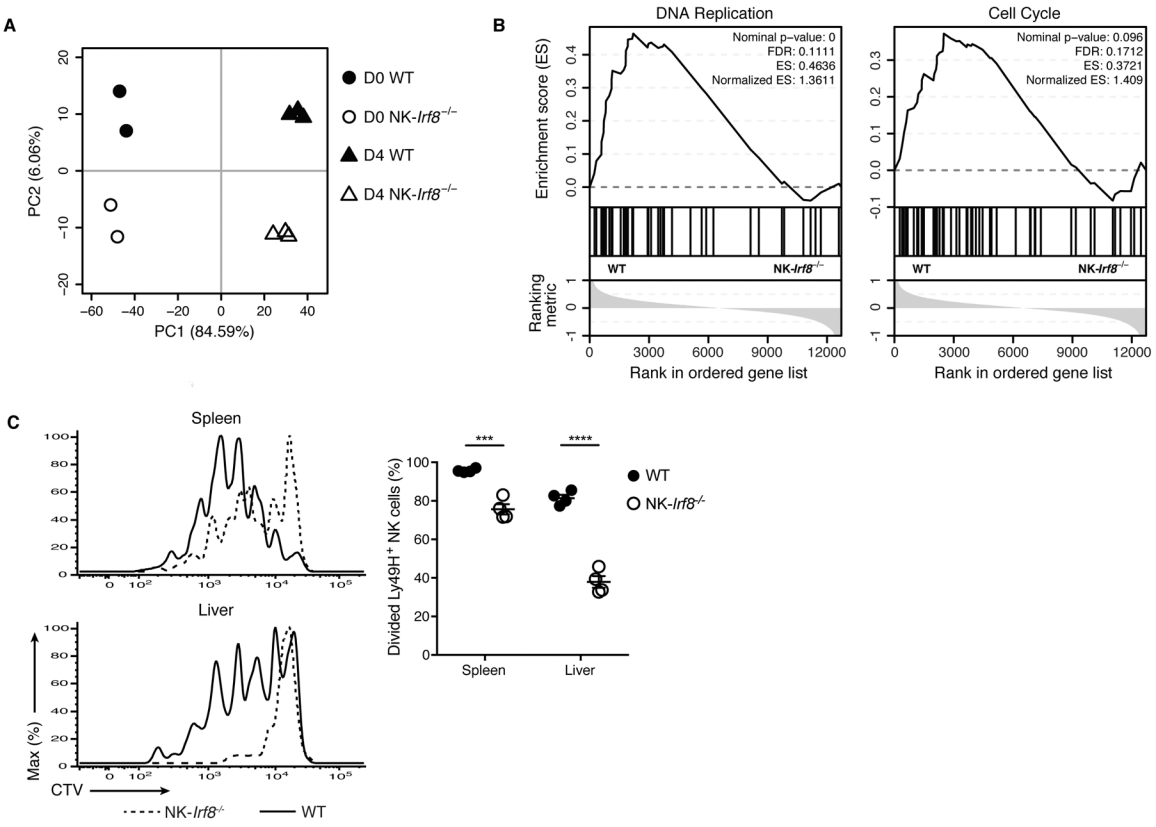

Figure 5. IRF8 drives a transcriptional program that promotes NK cell proliferation

(**A-B**) Mixed bone marrow chimeric mice harboring both WT and NK-*Irf8*$^{-/-}$ NK cells were infected with MCMV. Splenic Ly49H^{+} WT and NK-*Irf8*$^{-/-}$ NK cells were sorted for RNA-seq at day 0 and 4 p.i. (2–3 replicates per genotype and time point). (A) Principal component analysis of RNA-seq data, using the top 2000 genes with the highest variance. Each dot represents an RNA sample from a single mouse. (B) Gene set enrichment analysis of RNA-seq data at day 4 p.i. Genes within each given gene set are derived from significantly overrepresented PANTHER pathways and have expression above a minimal threshold based on the distribution of all genes.

(**C**) Experimental design as in Figure 4A, except NK cells were labeled with CTV prior to adoptive co-transfer. Representative histograms of CTV in splenic and hepatic WT and NK-*Irf8*$^{-/-}$ Ly49H^{+} NK cells at day 3 p.i. (left panel). Quantification of Ly49H^{+} NK cells that have divided at least once (right panel). Data are representative of two independent experiments with 4 mice per experiment. Groups were compared using an unpaired, two-tailed Student's t test. Data are presented as the mean ± SEM. ***$p < 0.001$, ****$p < 0.0001$. See also Figure S6 and Table S1.

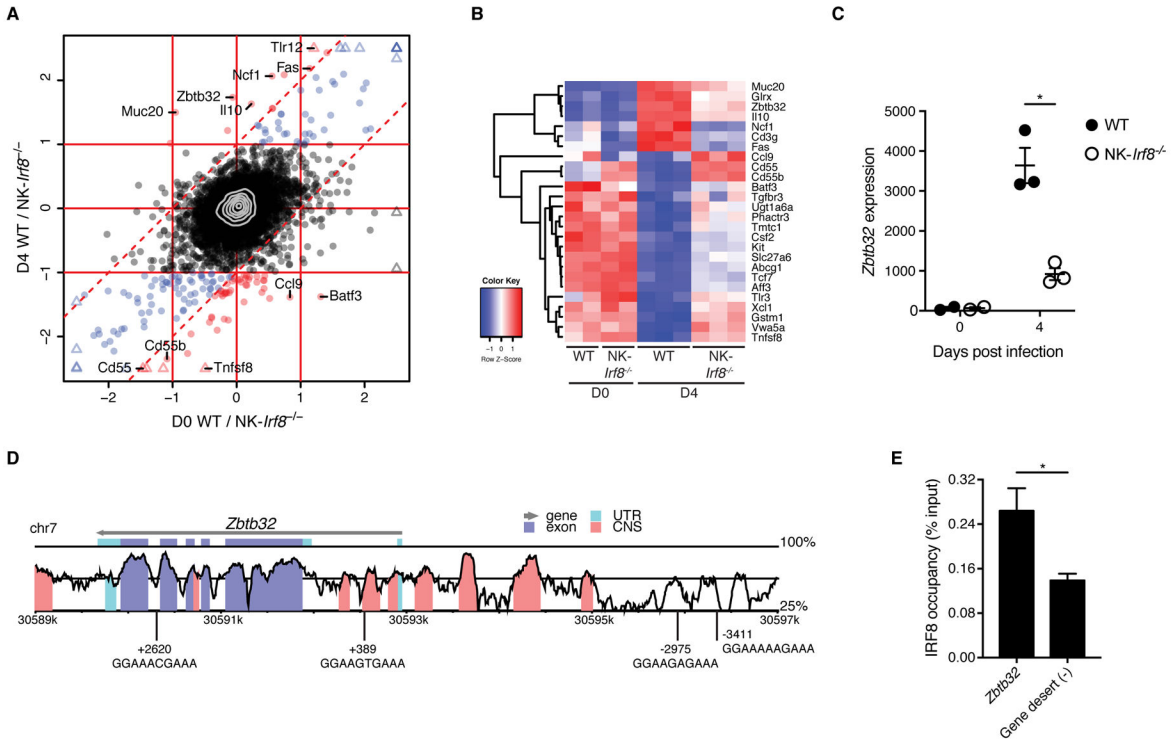

Figure 6. IRF8 directly regulates the pro-proliferative factor *Zbtb32*

(**A-C**) Experimental design as in Figure 5A. (A) Relative expression of all "expressed" genes in WT versus NK-*Irf8*$^{-/-}$ NK cells at day 4 p.i. compared with prior to infection. Red- or blue-colored dots denote | $D4_{Log2FC}$ | ≥ 1, and red dots specifically denote $D4_{Log2FC}$ − $D0_{Log2FC}$ ≥ 1 or $D4_{Log2FC}$ − $D0_{Log2FC}$ ≤ −1, i.e. genes which show greater differential expression between WT and NK-*Irf8*$^{-/-}$ at D4 than at D0. Triangles signify genes that have been coerced onto the plot boundary. (B) Heat map and hierarchical clustering of selected genes. Replicates are shown in order. Selected genes show greater differential expression in WT than in NK-*Irf8*$^{-/-}$ NK cells and at D4 more than at D0. (C) RNA-seq reads mapping to *Zbtb32* locus. P value was calculated in DESeq2 and adjusted for testing multiple hypotheses.

(**D**) Position and sequence of putative IRF8 binding sites are shown relative to *Zbtb32* promoter. Traces show percent conservation between mouse (mm10) and human (hg19) genomes. Conserved non-coding sequences (CNS) are defined as having >70% homology over >100bp. The location relative to the transcriptional start site and the sequence of the putative IRF8 motif are listed for each putative IRF8 binding site.

(**E**) Sorted splenic NK cells were stimulated with IL-2, IL-12, IL-15, and IL-18 for 16 hours. IRF8-DNA complexes were immunoprecipitated, followed by qPCR to amplify across a putative IRF8 binding site 2975 bp upstream of the *Zbtb32* promoter. A gene desert ~50kb upstream of the *Foxp3* locus served as a negative control for IRF8 binding. Data are representative of two independent experiments. Samples were compared using an unpaired, two-tailed Student's t test.

Data are presented as the mean ± SEM. *p < 0.05. See also Figure S6 and Table S1.